The Structural Characteristics of *Bombyx mori* Silk Fibroin before Spinning As Studied with Molecular Dynamics Simulation

Tsutomu Yamane, Kôsuke Umemura, and Tetsuo Asakura*

Department of Biotechnology, Tokyo University of Agriculture and Technology, Koganei, Tokyo 184-8588, Japan

Received June 17, 2002

ABSTRACT: In an initial attempt to understand the structural organization of *Bombyx mori* silk fibroin stored in the silk gland using several solid-state NMR techniques, we recently reported the conformation of the crystalline form of silk I (The unprocessed conformation of the silk fibroin before spinning in the solid state) as a repeated type II β-turn structure (Ala, $(\phi,\psi) = (-60°,130°)$, and Gly, $(\phi,\psi) = (70°,30°)$) in a model peptide $(Ala\text{-}Gly)_{15}$ (Asakura et al. *J. Mol. Biol.* **2001**, *306*, 291−305). To examine the favorable secondary structure(s) associated with silk fibroin molecules, we analyzed the results of molecular dynamic (MD) simulations of three model dipeptides of the type Ac-Xxx-NHMe (where Xxx = Gly, Ala and Ser) in *explicit* water because the concentration of the silk fibroin before spinning in the middle silk gland is about 30% in water. The conformational probability maps constructed for these dipeptides indicate that the torsion angles of Gly, Ala, and Ser residues in the type II β-turn structure are in the stable state even in water, and only our model among silk I models proposed previously can satisfy the stable state for these residues simultaneously. The high possibility of the appearance of β-turn structure is pointed out by the MD simulation of $Ac\text{-}(Ala\text{-}Gly)_8\text{-}NHMe$ molecule in water. There is also a high possibility to form intramolecular hydrogen bonding involving the ith Ser $O^{\gamma}H$ functionality as a donor and the $(i-3)$th Gly C═O group as an acceptor when the side chain conformation of the Ser residue, $\chi_1 = -60°$. This is derived from the molecular mechanics simulation of Ac-(Ala-Gly-Ser)-NHMe without water and will further stabilize the type II β-turn conformation.

Introduction

The conformational analysis of natural silk fibroin molecules has received considerable attention due to their excellent mechanical properties.[1] It is remarkable that silk fibroin from *Bombyx mori* silkworms can produce strong and tough fibers "naturally" from an aqueous solution at room temperature. On the other hand, synthetic materials with comparable elasticity and toughness usually require processing at higher temperatures and/or from less benign nonaqueous solvents.[2] To emulate the characteristics of such biomaterials, it is important to understand the conformations and structural organization of the silk fibroin molecules stored in silkworm, so that the design and development of silklike materials with desired functional properties can be produced under mild conditions.

The primary structure of the crystalline region of *B. mori* silk fibroin, largely consists of repetitive hexameric units: $(Gly\text{-}Ala\text{-}Gly\text{-}Ala\text{-}Gly\text{-}Ser)_n$.[3−6] The two distinct structural forms of the crystalline domains in *B. mori* silk fibroin are silk I and silk II (the structure of silk fiber after spinning), which have been characterized experimentally and theoretically employing X-ray diffraction,[3,7−14] electron diffraction,[11−14] infrared[15−17] and solid-state NMR spectroscopic techniques,[15,18−26] and conformational energy calculations.[12,27] The silk II structural form of the silk fiber has been characterized as an antiparallel β-sheet structure.[3,7,9,12,22−26] However, despite a long history of interest in the less stable silk I form, its structure has remained poorly understood[8,10−20,27] until recently.[28,29] Attempts to induce orientation of the silk I form for studies by X-ray diffraction, electron diffraction, or solid-state NMR easily causes its conversion to the more stable silk II form. Therefore, most of the investigations of the structure of the silk I form have been confined to a "modular approach" using synthetic peptides having repetitive natures, i.e., a $(Ala\text{-}Gly)_n$ sequence. However, the comparison of the conformations of these models, with limited experimental data, in fact resulted in a number of conflicting models proposed for the silk I structure.[8,10−20,27]

Most recently, we proposed a comprehensive model for silk I as a repeated β-turn type II structure, based on several solid-state NMR techniques including 2D spin diffusion, REDOR, and the characteristic ^{13}C chemical shift data, for a sequential 30 residue model peptide: $(Ala\text{-}Gly)_{15}$.[28,29] When unprocessed silk fibroin, obtained directly from the silk gland, is allowed to dry, the structure is referred to as silk I in the solid state. This does not mean that all of the conformation of the silk fibroin is silk I. Namely, only the crystalline domains such as $(GAGAGS)_n$ in the silk fibroin take the silk I structure and other domains take a distorted structure.[30,31] It may be noted that the concentration of the silk fibroin before spinning, in solution in the middle silk gland, is about 30% in water. The high concentration of "water" might be expected to have a strong influence on correlation between the silk I structure and the solution structure of the silk fibroin stored in the silk gland, which may reflect its strong association and/or interaction with water molecules.[32−35]

Over the decades, theoretical conformational analyses of simple model diamides Ac-Xxx-NHMe or For-Xxx-NH_2, bearing the side chains of proteinogenic amino acids, have provided much insight on the topological descriptions of the preferred backbone as well as side chain conformations in proteins and polypeptides par-

* Correspondence to: Tetsuo Asakura. Telephone and Fax: +81-42-383-7733. E-mail Asakura@cc.tuat.ac.jp.

10.1021/ma0209390 CCC: $22.00
Published on Web 10/05/2002

ticularly, in absence of nearest-neighbor and long-range interactions. Theoretical studies performed on model dipeptides, For-Xxx-NH_2 or Ac-Xxx-$NHCH_3$ (where Xxx = Gly, L-Ala or L-Ser), by molecular mechanics (MM)[36−50] and ab initio SCF methods have been reported.[51−56] The conformational potential energy surface $E(\phi,\psi)$ of these three model systems were remarkably different, indicating the relative importance and influence of stereochemical nature of the side chains in dictating the preferred backbone conformations. However, the (ϕ,ψ) torsion angles corresponding to the γ-turn conformation (C_{7eq}: $\phi \sim -82 \pm 2°, \psi \sim 70 \pm 6°$) were found to be invariably the energetically most stable. In addition, molecular dynamics (MD) simulations are extremely useful in predicting the structural changes.[57] However, the predicted results still depend on the nature of force fields used in the MD calculation. For example, it has been suggested that "several shallow minima corresponding to secondary structure disappear at the higher level theory", so it seems important to accumulate examples which could predict the experimental data well by the MD approach. In addition to the simplest achiral Gly residues, Ala and Ser are the most abundant chiral residues with a hydrophobic methyl and polar CH_2OH side chains, respectively, in *B. mori* silk fibroin. Therefore, it would be appropriate to examine the results of MD simulations performed on relevant model dipeptides and test their secondary structure formation in *B. mori* silk fibroin.

In this paper, to examine the repeated type II β-turn structure for silk I proposed by us, [28,29] MD simulation is performed for the model dipeptides Ac-Xxx-NHMe (Xxx = Gly, Ala, or Ser) in *explicit* water, considering the fact that, in addition to the intrinsic features of the precise primary structure, hydration can play a significant role. MD simulations on the components of proteins may reveal the role of water, and the conformational probabilities of these model dipeptides permitted us to evaluate and define qualitatively the local conformational space in the Ramachandran maps and presumably the water-mediated folding−unfolding process of the fibroin molecules in the native state. The appearance of β-turn structure in a longer silk model peptide chain, Ac-$(Ala\text{-}Gly)_8$-NHMe in water is also examined with the MD simulation in water. Moreover, the possibility of intramolecular hydrogen bonding through the OH group of Ser residue which further stabilizes the type II β-turn conformation in the solid state is studied with the MM simulation of Ac-(Ala-Gly-Ser)-NHMe in vacuo.

Calculations

All MD simulations were performed on SGI ORIGIN 200 workstation using the AMBER force field (parm94),[58] AMBER6 version.[59]

MD Simulation of Model Dipeptides in Water. MD simulations of the model dipeptides, Ac-Xxx-NHMe, (where Xxx = Gly, Ala, or Ser), were performed in *explicit* water at room temperature by placing them in the center of a box of the size (20 × 20 × 20 Å) surrounded by water molecules having a density of 1.0 g cm^{-3}. Each system contained about 300 water molecules. Water molecules that overlapped with the peptide atoms were eliminated. The TIP3P water model described by Jorgensen et al. was used.[60] The simulations were performed uniformly with periodic boundary conditions and with an *NVT* ensemble. The nonbonded energies and forces were approximated using the cutoff distance of 10 Å, which were processed using a list-based algorithm that was updated every 10 steps. All of simulations were run for 5 000 000 steps, and structural data were sampled every 50 steps. In total, 100 000 frames of structural data were sampled during each trajectory in the simulation. The leapfrog algorithm was used to integrate Newton's equations of motion (with a time step of 1.0 fs). Temperature was controlled at 300 K by using Berendsen's weak coupling heat bath[61] and a step size of 1fs. Backbone torsion angles (ϕ,ψ) were extracted from the trajectory of each simulation and used for calculation of histograms of the number of conformers $N(\phi \pm 10°, \psi \pm 10°)$, where $N(\phi \pm 10°, \psi \pm 10°)$ means the number of conformers with torsion angles: $(\phi \pm 10°, \psi \pm 10°)$. The conformational probability $P(\phi,\psi)$ of Ala and Gly dipeptides were obtained from the following equation[35]

$$P(\phi,\psi) = \frac{N(\phi \pm 10°, \psi \pm 10°)}{N_{\text{total}}} \tag{1}$$

where N_{total} means total number of frames in the trajectory $N_{\text{total}} = 100\,000$. The conformational probability maps were produced based on $P(\phi,\psi)$.

The side-chain conformation of the Ser residue has an effect on stability of the backbone conformation. In fact, some studies of Ser's backbone conformation did consider such a side-chain effect.[53] Here, we ran nine series of MD simulations. These simulations were performed under the constraint of side chain conformations χ_1 and χ_2, with three types of stable conformation, gauche (60°), trans (180°), and gauche′ (−60°): (χ_1,χ_2) = (60°,60°), (60°,180°), (60°,−60°); (180°,60°), (180°,180°), (180°,−60°); and (−60°,60°), (−60°,180°), (−60°,−60°), respectively. From the results of these simulations, the $P(\phi,\psi)$ map of Ser dipeptide was obtained using the following equation:

$$P(\phi,\psi) = \sum_{\chi_1}\sum_{\chi_2} P(\chi_1,\chi_2) P_{\chi_1,\chi_2}(\phi,\psi) \tag{2}$$

Here, $P(\chi_1,\chi_2)$ is defined as follows:

$$P(\chi_1,\chi_2) = \frac{1}{Z} \exp\{-\beta\langle E(\chi_1,\chi_2)\rangle\} \tag{3}$$

$$Z = \sum_{\chi_1,\chi_2} \exp\{-\beta\langle E(\chi_1,\chi_2)\rangle\} \tag{4}$$

Here $\beta = 1/kT$, $\langle E(\chi_1,\chi_2)\rangle$ is the average potential energy of a series of MD simulations with any couple of (χ_1,χ_2), and Z is the partition function of $P(\chi_1,\chi_2)$. Here, $<E(\chi_1,\chi_2)>$ is defined as follows:

$$\langle E(\chi_1,\chi_2)\rangle = \langle E_{\text{p-p}}(\chi_1,\chi_2)\rangle + \langle E_{\text{p-w}}(\chi_1,\chi_2)\rangle \tag{5}$$

where $\langle E_{\text{p-p}}(\chi_1,\chi_2)\rangle$ is the average of potential energy between intradipeptide atoms and $\langle E_{\text{p-w}}(\chi_1,\chi_2)\rangle$ is the average of potential energy between water and dipeptide atoms.

MD Simulation of Ac-$(Ala\text{-}Gly)_8$-NHMe in Water. MD simulations of a longer peptide, Ac-$(Ala\text{-}Gly)_8$-NHMe, embedded in *explicit* water molecules at room temperature were performed for 350 ps (350 000 steps). In this calculation, the "cap" option for treatment of water molecules on AMBER program, which generates the *explicit* water model spherically, was used, and the

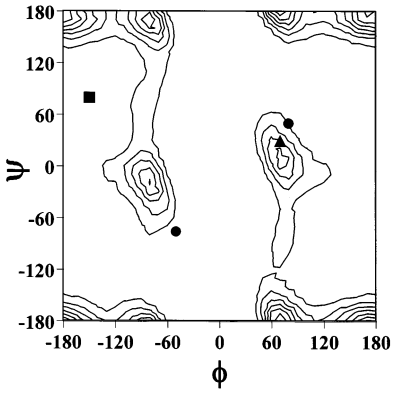

Figure 1. Conformational probability map of glycine dipeptide, Ac-Gly-$NHCH_3$, in water. Contour lines were drawn between $0.001 \leq P(\phi,\psi) \leq 0.01$ for every 0.001. The marks plotted on the map are conformations of silk I models proposed previously; ▲, ●, and ■ mean our model,[28] the crank shaft model,[11] and the out-of-register model,[27] respectively.

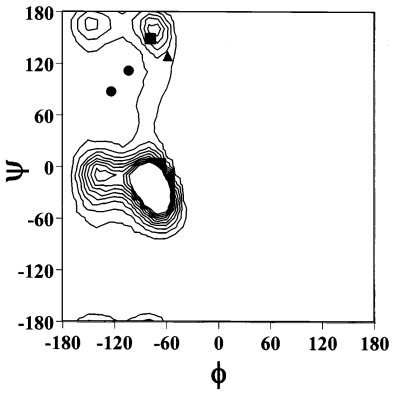

Figure 2. Conformational probability map of alanine dipeptide, Ac-Ala-$NHCH_3$, in water. Contour lines were drawn between $0.001 \leq P(\phi,\psi) \leq 0.01$ for every 0.001. The marks plotted on the map are conformation of silk I models proposed previously; ▲, ●, and ■ mean our model,[28] the crank shaft model,[11] and the out-of-register model,[27] respectively.

center of mass of solute molecules was placed in the center of mass of the spherical water molecule cluster. The radii of spherical water cluster was defined as 30 Å (total number of water molecules is 3600), which is large enough to cover solute molecules with every conformations. To avoid the contibution of the vapor of the water molecules to the out of water molecule cluster, harmonic potential (force constant; 6.28 (kJ/Å^2)) was applied to water molecules placed on surface of spherical water cluster. Other computational conditions were similar to the above-mentioned MD calculation for dipeptides in water.

MM Calculation of Ac-Ala-Gly-Ser-NHMe in Vacuo. MM calculations of Ac-Ala-Gly-Ser-NHMe in a type II β-turn conformation were performed with the same force field of the MD simulations as functions of χ_1 and χ_2 of the Ser side chain for each 120° intervals. These calculations were performed in vacuo, and the energies were minimized by 100 steps of the steepest decent method.

Results

The Conformational Characteristics of Ac-Gly-NHMe in Water. Figure 1 shows the ϕ,ψ conformational probability contour plot for the nonchiral Gly dipeptide Ac-Gly-NHMe in water. The high probability regions are largely symmetric, through the (0°,0°) origin, in the Ramachandran map. The plot contains three unique minima with relatively high probabilities in the area ($\phi = -180$ to 0°,$\psi = -180$ to 180°), defined as C_5, 3_{10}-helical region, and polyproline type II (P_{II}) conformations, characterized by the torsion angles ($\phi = -180°,\psi = 180°$), ($\phi = -80°,\psi = -20°$), and ($\phi = -80°,\psi = 170°$), respectively. The relative stabilities of these conformations follow the order $C_5 \approx \geq 3_{10} > P_{II}$. Because the high probability regions are largely symmetric, the regions characterized by the torsion angles ($\phi = 180°,\psi = -180°$), ($\phi = 80°,\psi = 20°$) and ($\phi = 80°,\psi = -170°$) are also three unique minima with relatively high probabilities in the region ($\phi = 0°-180°,\psi = -180°-180°$). The predicted backbone torsion angles of the Gly residue ($\phi = 70°,\psi = 30°$, Figure 1 (▲)), located in one of the high probability regions, are indeed accommodated in our proposed model of silk I structure.[28]

The Conformational Characteristics of Ac-Ala-NHMe in Water. The conformational probability contour (ϕ,ψ) plot is shown for Ala dipeptide, Ac-Ala-NHMe, in water (Figure 2). The regions have been called C_5, α_R, and P_{II} and the center of each region is (ϕ,ψ) = (−150°,170°), (−70°,−20°), and (−70°,160°), respectively. The most stable structure appeared in the α_R region (typical α_R helix is (ϕ,ψ) = (−57°, −47°)). The torsion angles of Ala residue in our proposed silk I model were (ϕ,ψ) = (−60°,130°) (Figure 1 (▲)), which belong to the P_{II} region. The main difference in the torsion angles between α_R and P_{II} is the ψ angle, rather than the ϕ angle. The comparison of the present results with MD calculation and previous results for Ac-Ala-NHMe will be discussed in the Discussion.

The Conformational Characteristics of Ac-Ser-NHMe in Water. Figure 3 shows the conformational probability contour (ϕ,ψ) plot for Ser dipeptide, Ac-Ser-NHMe, in water, with different side chain conformations (χ_1 and χ_2), as depicted in the methodology of MD simulation. All of the plots contain three major high-probability regions α_R, P_{II}, and C_5. However, the relative stability among their conformations is different depending on the side chain conformation. Figure 4 is the conformational probability map accounting for the effect of the conformation of the side chain by using eq 2. As described above, the stability of backbone conformations of Ser dipeptide depends on the side chain conformation. Therefore, the intramolecular hydrogen bonds formed between the side-chain O^γ and backbone amide proton or between the side-chain H^γ and backbone carbonyl oxygen in Ser residue might be a major reason for such differences in the conformational stability between Ala and Ser residues. The atom pairs that could form intramolecular hydrogen bonding within one Ser dipeptide molecule are as follows; (A) Ac C*O*-Ser H^γ, (B) Ser N*H*-Ser O^γ, (C) Ser H^γ-Ser C*O* and (D) Ser O^γ-N*H*Me. The average distances calculated for the atomic pair (A) to (D) for different side chain conformations are summarized in Figure 5. There are no atomic pair whose distance is less than 2.5 Å. Thus, the contribution of intramolecular hydrogen bonding to the stability of Ser dipeptide is likely small. The probabilities of C_5, P_{II}, and α_R regions and their differences in free energy for Ala, Gly, and Ser dipeptides calculated here are summarized in Table 1.

The Conformational Characteristics of Ac-(Ala-Gly)$_8$-NHMe in Water. The aspect of β-turn appearance was studied with MD calculation for a longer chain of the model peptide of silk fibroin, an Ac-(Ala-Gly)$_8$-

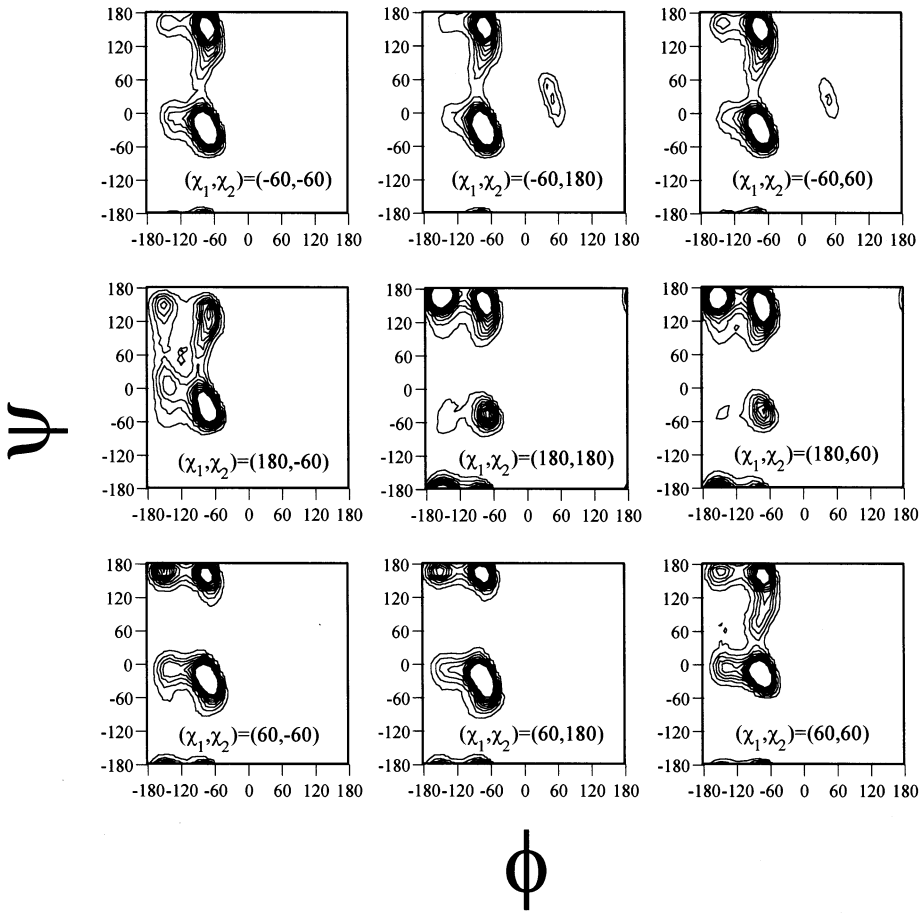

Figure 3. Conformational probability maps of serine dipeptide,Ac-Ser-$NHCH_3$, with nine possible pairs of side chain conformations (χ_1 and χ_2). Contour lines were drawn $0.001 \leq P(\phi,\psi) \leq 0.01$ for every 0.001.

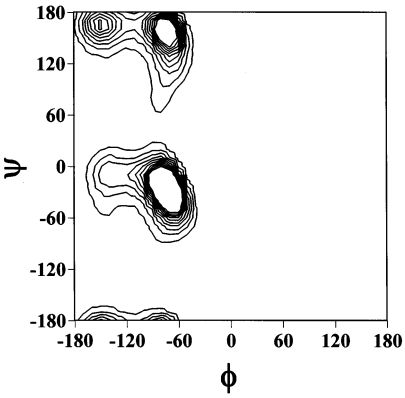

Figure 4. Conformational probability map of serine dipeptide, Ac-Ser-$NHCH_3$, averaged over nine side chain conformations in water according to eq 2 in the text.

NHMe molecule in water. Figure 6 shows a plot of the number of Ala-Gly pairs in Ac-$(Ala\text{-}Gly)_8$-NHMe with β-turn type II structure by means of MD simulation in water. Here the starting structure was β-turn type II structure determined by us previously:[28] (Ala, $(\phi,\psi) = (-60°,130°)$. and Gly. $(\phi,\psi) = (70°,30°)$). The ϕ,ψ angles (Ala, $(\phi,\psi) = (-60° \pm 30°,130° \pm 30°)$, and Gly, $(\phi,\psi) = (70° \pm 30°,30° \pm 30°)$) were selected as the possible β-turn structures during the MD simulation. The appearance and disappearance of β-turn structure occur during the MD simulation in water. The β-turns, turns 4 and 5, in the central parts tend to disappear within short time. On the other hand, the β-turns, 3 and 6, which are adjacent to the central β-turns, 4 and 5, tend to keep the structure during the MD simulation.

The Conformational Characteristics of Ac-Ala-GlySer-NHMe in Vacuo. To examine the proposed type II β-turn structure in the solid state, it is interesting to consider the possibility of the additional formation of an intramolecular hydrogen bond through the OH group of the Ser side chain and the backbone C═O group in the β-turn structure of the backbone chain. Thus, the MD calculation was also performed for the Ac-AlaGly-Ser-NHMe molecule with $(\phi,\psi) = (-60°,130°)$ for Ala and Ser residues and $(\phi,\psi) = (70°,30°)$ for the Gly residue by changing both the χ_1 and χ_2 angles of the side chain of Ser residue as trans (180°), gauche (60°), and another gauche (−60°) in vacuo. Here, the β-turn type II structure of the backbone chain was formed between Ac C═O and Ser NH groups. Figure 7 shows that the most stable state of the Ser side chain is $(\chi_1,\chi_2) = (-60°,-60°)$ although the side chain conformations with $\chi_1 = -60°$ are relatively stable, independent of the χ_2 values. When the side chain conformation $(\chi_1,\chi_2) = (-60°,60°)$, the intramolecular hydrogen bond is formed between the OH of the Ser side chain and the backbone Ac C═O group as well as the intramolecular hydrogen bond between Ac C═O and Ser NH groups as shown in Figure 8.

Discussion

The Conformational Properties of Ala and Gly Residues of *B. mori* Silk Fibroin. Over the past few decades, the alanine dipeptide has been studied about its conformational equilibria *in aqueous* solution or in

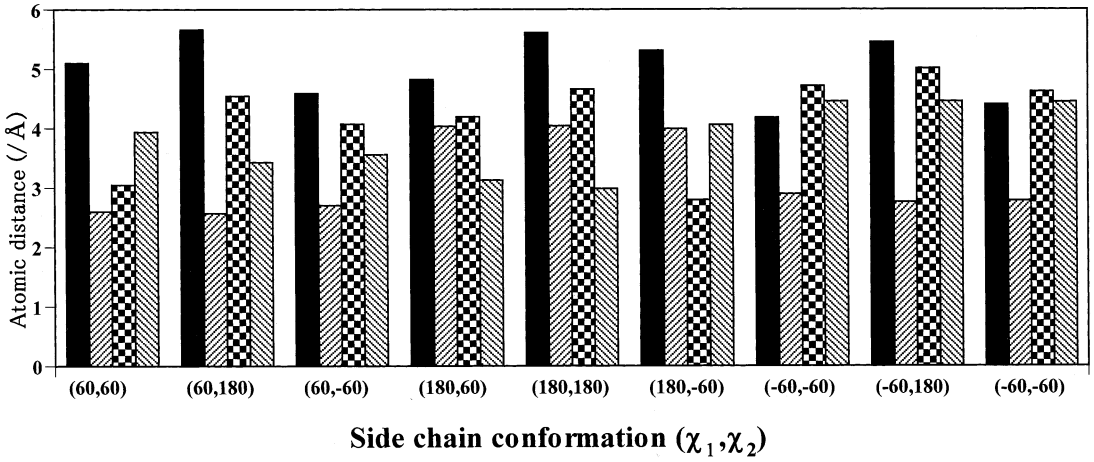

Figure 5. Atomic distances of three pairs of atoms in serine dipeptide Ac-Ser-$NHCH_3$ which form hydrogen bonds in nine side chain conformations (from left to right) Ac*CO*-Ser *Hγ* (■), Ser N*H*-Ser *Oγ* (right slants), Ser *Oγ*-N*H*Me (checkerboard shading), and Ser *Hγ*-Ser C*O* (left slants) after MD simulation.

Table 1. Conformational Probabilities of the Energetically Stable Regions

	conformational (ϕ,deg,ψ,deg)/probability[a] ($\Delta\Delta G_X$, kJ/mol)[b]		
model peptide	C_5	P_{II}	α_R
Ac-Ala-$NHCH_3$	(−150,170)/0.0555 (0)	(−70,160)/0.0843 (−1.042)	(−70,−20)/0.450 (−5.220)
Ac-Gly-$NHCH_3$	(−180,180)/0.1611 (0)	(−80,170)/0.1036 (1.151)	(−80,−20)/0.1016 (1.101)
Ac-Ser-$NHCH_3$	(−150,160)/0.1310 (0)	(−70,160)/0.2148 (−1.235)	(−70,−30)/0.3720 (−1.620)

[a] Conformational probability $P(\phi'' \pm 30°,\psi'' \pm 30°)$ is calculated by the following equation:

$$P(\phi \pm 30°,\psi \pm 30°) = \sum_{\substack{\phi - 30° \le \phi' < \phi - 30°, \\ \psi - 30° \le \psi' < \psi - 30°}}$$

Here, (ϕ'',ψ'') is the maximum point of the conformational probability map, for C_5, P_{II}, and α_R. [b] $\Delta\Delta G_X$ is the free energy of conformation X relative to C_5, calculated by the following equation: $\Delta G_X = -RT \ln(P_X/P_{C5})$. Here P_X and P_{C5} are the probabilities of conformations X and C_5, respectively.

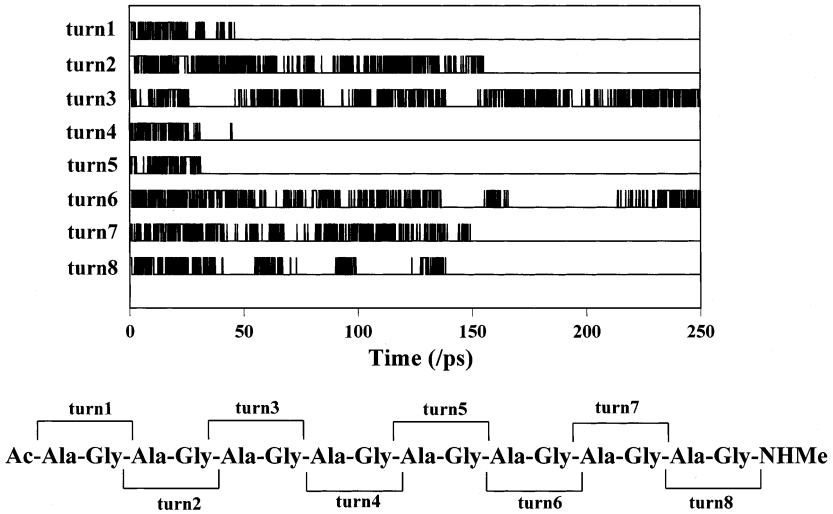

Figure 6. Plot of number of Ala-Gly pairs in Ac-(Ala-Gly)$_8$-NHMe with *β*-turn type II structure by means of MD simulation in water. Here the starting structure was *β*-turn type II structure determined by us previously (Ala, $(\phi,\psi) = (-60°,130°)$, and Gly, $(\phi,\psi) = (70°,30°)$). The ϕ,ψ angles within ±30° were selected for Ala and Gly residues as the *β*-turn structure during the MD simulation. The appearance of the *β*-turn structure was shown as vertical bow.

vacuo theoretically. Many of theoretical studies about alanine dipeptide are summarized in a review of Brooks and Case.[62] In quantum mechanical study, many calculations on the alanine dipeptide have been attempted; Ab initio calculation of conformational energy of the alanine dipeptide at some spacing in ϕ,ψ with a Hartree−Fock (HF) 3-21G, HF/DZP, HF/6-31+G*, and HF/6-311G** basis set, and its results are summarized elsewhere[44,54−56] These results suggest that the stability of local minima in vacuo is $C_7^{eq} > C5 > C_7^{ax} > \alpha_R$ with energy differences relative to C_7^{eq} about 4−8, 8−9, and 17−21 kJ/mol, respectively. On the other hand, in the molecular mechanics study, some of calculations used to obtain the adiabatic energy surface in vacuo for the several force fields (ECEPP/2, AMBER, CHARM19, etc.) have been performed.[36−42] The general features of the results with these force fields are nearly the same as those for the Hartree−Fock surface, except for ECEPP

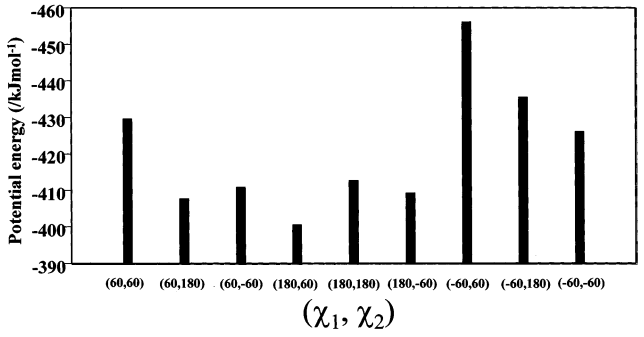

Figure 7. Conformational energies of Ac-AlaGlySer-NHMe molecule with $(\phi,\psi) = (-60°,130°)$ for Ala and Ser residues and $(\phi,\psi) = (70°,30°)$ for the Gly residue by changing both the χ_1 and χ_2 angles of the side chain of Ser residue as trans (180°), gauche (60°), and another gauche (−60°) in vacuo. Here, the β-turn type II structure was formed between Ac C═O and Ser NH groups.

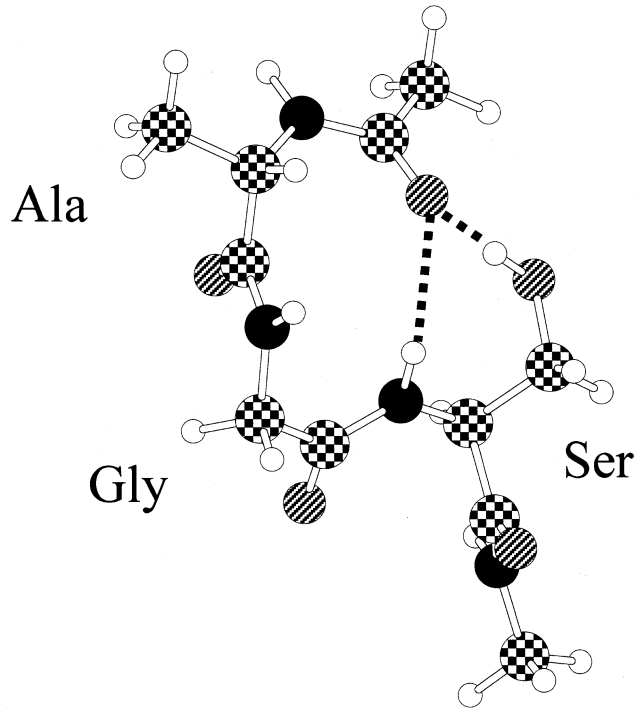

Figure 8. View of the most stable state of AcAlaGlySerNHMe molecule with $(\phi,\psi) = (-60°,130°)$ for Ala and Ser residues and $(\phi,\psi) = (70°,30°)$ for the Gly residue. The side chain conformation of the Ser residue is $(\chi_1,\chi_2) = (-60°,60°)$, where the intramolecular hydrogen bond is formed between the OH of the Ser side chain and the backbone Ac C═O group as well as the intramolecular hydrogen bond between Ac C═O and Ser NH groups.

potentials, which give different relative energies of the local minima compared with other force fields. Additionally, free energy estimation studies in vacuo[44] and in aqueous solution[43,45−49] based on external RISM integral equation approach coupled with Monte Carlo free energy simulation,[45,46] molecular dynamics-based free energy methods,[47] Poisson−Boltzmann methods coupled with OPLS[48] and CHARMM[49] and molecular mechanics coupled with reaction field arising from solvent represented as a surface charge density at the solvent-accessible surface[43,50] have been attempted. From these studies, two general features are observed. Namely, α_R region of conformation space is significantly stabilized, and local energy regions become broader than those of in vacuo results. And, in aqueous solution, P_{II} becomes primary or secondary stable region.

In our study, we attempted to obtain conformational probability map of dipeptide model (Ac-X-NHMe, X = Ala, Gly, Ser) through long time molecular dynamics simulation embedded in explicit water molecules. This is a rare case study using molecular dynamics simulation of the explicit water solution system directly to obtain the conformational probability map because this method is difficult to hold ergodicity. Thus, to confirm the reliability of our simulation, we attempted the molecular dynamics simulation of Ala and Gly dipeptides, which have been well-known about the property of conformational stability in aqueous solution. Thus, we can use the conformational probability contour (ϕ,ψ) maps for discussing the local conformation of silk fibroin in water. Although silk I is the structure of *B. mori* silk fibroin before spinning in the solid state, this is expected to correlate strongly with the silk fibroin structure in water because the silk fibroin in a silk I form is prepared from silk fibroin stored in the silk gland and dried gently. In Figures 1 and 2, the conformations of previous silk I models, crankshaft model[11] and out-of-register model[27] are marked together with our silk I model. In Figure 2, the torsion angles of Ala residue in the out-of-register model and our β-turn type II model are in the region of P_{II}, but those of two kinds of crankshaft models are in the less stable region. On the other hand, the torsion angle of the Gly residue is in our β-turn type II model and one of two kinds of crankshaft models. Thus, only the torsion angles of Ala and Gly residues of our silk I model can satisfy the stable states, simultaneously, in the conformational probability maps of Ala and Gly residues. However, the most stable state of the Ala residue calculated by the MD method is the α_R region. Figure 2 indicates the high possibility of appearance of the structure in the α_R region for Ala residues of silk fibroin chains in water. The plot for the Gly residue shown in Figure 1 indicates appearance of the regions of −60° for ϕ and −60° to 60° for ψ other than the region with torsion angle of Gly residue $(\phi,\psi) = (70°,30°)$. As reported previously,[63−66] the ^{13}C chemical shifts of Cα, Cβ and CO carbons of Ala residues of *B. mori* silk fibroin, in the isolated silk gland and also even in living silkworm are clearly different from the corresponding Ala chemical shifts of α-helix. Namely, the chemical shifts of Ala residues of silk fibroin stored in the silk gland of *Samia cynthia ricini* become a measure of α-helix chemical shift because poly(alanine) in the silk fibroin clearly takes the α-helix in silk gland. The chemical shifts of three Ala carbons of *B. mori* silk fibroin are quite different from the α-helix chemical shifts and close to the random coil chemical shifts of Ala residues in proteins and Ac-Ala-$NHCH_3$ in water. Thus, we can eliminate the α-helix conformation as the solution structure.[34,63−66] The observed CD spectrum of *B. mori* silk fibroin from the silk gland is characterized by the presence of poorly defined toughs, at ∼218 and ∼206 nm.[35,67] This CD pattern is distinctly different from the one usually attributed to proteins and polypeptides predominantly in an α-helical conformation. This spectrum can be interpreted with a mixture of type I β-turn (50%) and a random coil structure (50%) if we adopt the analysis by Perczel et al.[68] As summarized in Figure 6, the appearance and disappearance of β-turn structure occur during MD simulation in water. The β-turns, turns 4 and 5, in the central parts tend to

disappear within short time. On the other hand, the β-turns, 3 and 6, which are adjacent to the central β-turns, 4 and 5, tend to keep the β -turn structure during MD simulation. Thus, the mixture of β-turn and random coil seems valid as a conformational model of silk fibroin in aqueous solution.

In the present study, MD simulations assume very dilute aqueous solution. However, silk fibroin in the silk gland (called liquid silk) is present in the concentrated state, and therefore, we must consider the stability of the local conformation by taking into account aggregation effects. The ^{13}C spin−lattice relaxation times, T_1, of *B. mori* silk fibroin have been reported as a function of the concentration in water.[33,34] The T_1 values of all of the carbons decrease and the mean correlation times calculated from the T_1 values of the backbone carbons increase with increasing silk concentration. Thus, the aggregation of the silk fibroin molecules occurs with increasing concentration. In the proposed silk I conformation, β-turn, the C═O and NH bond direction other than the bonds contributing intramolecular hydrogen bonding is perpendicular to the backbone direction, and therefore, it is easy to form intermolecular hydrogen bonding.[28] Thus, in the silk gland, the conformational probability of Ala and Gly residues to form the type II β-turn may be enhanced. Actually, the observed CD pattern of silk fibroin in water at low concentration, ∼0.1%, indicates that the predominant structure is random coil/unordered structure.[35,67] However, the CD spectrum of *B. mori* silk fibroin from the silk gland (∼8.6%) is quite different and is characterized by the presence of poorly defined troughs, at ∼218 and ∼206 nm as mentioned above. We have reported the ^{1}H-coupled and -decoupled ^{13}C solution NMR spectra of the carbonyl for the Gly residue of [1-^{13}C]Gly-labeled silk fibroin in D_2O.[34] The observations of the long-range coupling constant between ^{13}C and ^{1}H nuclei, $^3J_{C'-N-C\alpha-H}$, are expected to reflect the local conformation. The value of the $^3J_{C'-N-C\alpha-H}$ was readily determined from the spacing of the doublet for each Gly carbonyl carbon peak in the ^{1}H-coupled spectra. After correction, by means of the peak-to-trough ratio of the doublet,[34] the $^3J_{C'-N-C\alpha-H}$ values were determined as follows: 2.8 Hz for the G−A−***G***−S−G sequence, 2.4 Hz for the G−S−***G***−A−G sequence, and 2.6 Hz for the G−A−***G***−A−G sequence at 1.8% w/v. These values decrease slightly with increasing concentration: 2.5 Hz for the G−A−***G***−S−G sequence, 2.0 Hz for the G−S−***G***−A−G sequence, and 2.2 Hz for the G−A−***G***−A−G sequences at 7.3% w/v. If the ϕ value of the Ala residue is ∼ −60°, which is a typical ϕ value with silk I structure, $^3J_{C'-N-C\alpha-H}$ can be calculated to be −0.75 Hz. Thus, the decrease in the long range coupling constant is expected if some amounts of silk I structure appears because the coupling constant reflects fast exchange among several conformations. These studies support the generation of ordered structure, namely β-turn structure rather than α-helix structure, with increasing silk concentration.

The Role of Ser Residue in the Structure of Silk Fibroin. The probability maps on Ramachandran (ϕ,ψ) plots of Ser dipeptide models indicate that the P_{II} region, which forms a part of type II β-turn conformation, is a secondary major conformational region of Ala and Ser residues in water. These results suggest that the silk I form may reflect conformational properties of the residues in water. Especially, as shown in Table 1, the P_{II} region of the Ser dipeptide is more stable than that of Ala dipeptide, which is consistent with results of solid-stateNMR.[31,35]

In the results of all series of MD simulation, α_R is the most stable conformation. Meanwhile, in the case of gauche' ($\chi_1 = -60°$), the side chain O^γ atom is relatively far from both the carbonyl carbon and amide proton. In this conformation, all of the hydrophilic atoms in the Ser dipeptide are easily accessible to water molecules. These results suggest that the formation of silk I structure of *B. mori* silk fibroin depends on the water and the major side chain conformation will be around −60°. As shown in Figure 8, the β-turn structure with type II is stabilized by the hydrogen bonds formed between ith Ser OH group and (i − 3)th Gly carbonyl group when the χ_1 angle of the Ser residue is around −60°. In globular proteins, Baker et al. suggested the existence of such hydrogen bond in β-turn or 3_{10}-helix structures.[69] Thus, the Ser residue with $\chi_1 = -60°$ in silk fibroin will stabilize the type II β-turn conformation through formation of intramolecular hydrogen bonding along the chain when water molecules were eliminated.

Acknowledgment. We acknowledge support from the Program for promotion of Basic Research Activities for Innovative Biosciences, Japan. We also acknowledge Dr. R. Kishore, who was a visiting researcher (JSPS Invitation Fellowship), for a useful discussion.

References and Notes

(1) Vollrath, F.; Knight, D. P. *Nature (London)* **2001**, *410*, 541−548.
(2) Asakura, T.; Kaplan, D. L. In *Encyclopedia of Agriculture Science*; Academic Press: New York, 1994; pp 1−11.
(3) Fraser, R. D. B.; MacRae, T. P. In *Conformations of Fibrous Proteins and Related Synthetic Polypeptides*; Academic Press: New York, 1973.
(4) Asakura, T.; Watanabe, Y.; Ito, T. *Macromolecules* **1984**, *17*, 2421−2426.
(5) Mita, K.; Ichimura, S.; James, T. C. *J. Mol. Evol.* **1994**, *38*, 583−592.
(6) Zhou, C.-Z.; Confalonieri, F.; Medina, N.; Zivanovic, Y.; Esnault, C.; Yang, T.; Jacquet, M.; Janin, J.; Duguet, M.; Perasso, R.; Li, Z.-G. *Nucleic Acids Res.* **2000**, *28*, 2413−2419.
(7) Marsh, R. E.; Corey, R. B.; Pauling, L. *Biochim. Biophys. Acta* **1955**, *16*, 1−34.
(8) Konishi, T.; Kurokawa, M. *Sen'I Gakkaishi* **1968**, *24*, 550−554.
(9) Takahashi, Y.; Gehoh, M.; Yuzuriha, K. *Int. J. Biol. Macromolecules* **1999**, *24*, 127−138.
(10) Anderson, J. P. *Biopolymers* **1998**, *45*, 307−321.
(11) Lotz, B.; Kieth, H. D. *J. Mol. Biol.* **1971**, *61*, 201−215.
(12) Lotz, B.; Cesari, F. C. *Biochimie* **1979**, *61*, 205−214.
(13) Okuyama, K.; Nakajima, Y.; Hasegawa, Y.; Hirabayashi, K.; Nishi, N. *J Seric. Sci. Jpn.* **1988**, *57*, 23−30.
(14) He, S.-J.; Valluzzi, R.; Gido, S. P. *Int. J. Biol. Macromolecules* **1999**, *24*, 187−195.
(15) Asakura, T.; Kuzuhara, A.; Tabeta, R.; Saito, H. *Macromolecules* **1985**, *18*, 1841−1845.
(16) Hayakawa, T.; Kondo, K.; Yamamoto, S.; Noguchi, J. *Kobunsi Kagaku* **1970**, *27*, 229−241.
(17) Magoshi, J.; Mizuide, M.; Magoshi, Y.; Takahashi, K.; Kubo, M.; Nakamura, S. *J. Polym. Sci., Polym. Phys. Ed.* **1979**, *17*, 515−520.
(18) Saito, H.; Iwanaga, Y.; Tabeta, R.; Narita, M.; Asakura, T. *Chem. Lett.* **1983**, 427−430.
(19) Saito, H.; Tabeta, R.; Asakura, T.; Iwanaga, Y.; Shoji, A.; Ozaki, T.; Ando, I. *Macromolecules* **1984**, *17*, 1405−1412.
(20) Asakura, T.; Yamaguchi, T. *J. Seric. Sci. Jpn.* **1987**, *56*, 300−304.
(21) Ishida, M.; Asakura, T.; Yokoi, M.; Saito, H. *Macromolecules* **1990**, *23*, 88−94.
(22) Nicholson, L. K.; Asakura, T.; Demura, M.; Cross, T. A. *Biopolymers* **1993**, *33*, 847−861.
(23) Asakura, T.; Aoki, A.; Demura, M.; Joers, J. M.; Rosanske, R. C.; Gullion, T. *Polym. J.* **1994**, *26*, 1405−1408.

(24) Asakura, T.; Demura, M.; Hiraishi, Y.; Ogawa, K.; Uyama, A. *Chem. Lett.* **1994**, 2249−2252.
(25) Asakura, T.; Minami, M.; Shimada, R.; Demura, M.; Osanai, M.; Fujito, T.; Imanari, M.; Ulrich, A. S. *Macromolecules* **1997**, *30*, 2429−2435.
(26) Demura, M.; Minami, M.; Asakura, T.; Cross, T. A. *J. Am. Chem. Soc.* **1998**, *120*, 1300−1308.
(27) Fossey, S. A.; Nemethy, G.; Gibson, K. D.; Sheraga, H. A. *Biopolymers* **1991**, *31*, 1529−1541.
(28) Asakura, T.; Ashida, J.; Yamane, T.; Kameda, T.; Nakazawa, Y.; Ohgo, K.; Komatsu, K. *J. Mol. Biol.* **2001**, *306*, 291−305.
(29) Asakura, T.; Yamane, T.; Nakazawa, Y.; Kameda, T.; Ando, K. *Biopolymer* **2001**, *58*, 521−525.
(30) Asakura, T.; Sugino, R.; Yao, J.; Takashima, H.; Kishore, R. *Biochemistry* **2002**, *41*, 4415.
(31) Asakura, T.; Sugino, R.; Okumura, T.; Nakazawa, Y. *Protein Sci.* **2002**, *11*, 1873.
(32) Asakura, T.; Suzuki, H.; Watanabe, Y. *Macromolecules* **1983**, *16*, 1024−1026.
(33) Asakura, T.; Watanabe, Y.; Uchida, A.; Minagawa, H. *Macromolecules* **1984**, *17*, 1075−1081.
(34) Asakura, T. *Makromol Chem.* **1986**, *7*, 755−759.
(35) Asakura, T.; Ashida, J.; Yamane, T. ACS Symposium Series 834, cap. 6, 2002.
(36) Zimmerman, S. S.; Pottle, M. S.; Némethy, G.; Scheraga, H. A. *Macromolecules* **1977**, *10*, 1−9.
(37) Nguyen, D. T.; Case, D. A. *J. Phys. Chem.* **1985**, *89*, 4020−4026.
(38) Pettitt, B. M.; Karplus, M. *J. Am. Chem. Soc.* **1985**, *107*, 1166−1173.
(39) Weiner, S. J.; Kollman, P. A.; Nguyen, D. T.; Case, D. A. *J. Comput. Chem.* **1986**, *7*, 230−252.
(40) Jorgensen, W. L.; Tirado-Rives, J. *J. Am. Chem. Soc.* **1988**, *110*, 1657−1671.
(41) Roterman, L. K.; Lambert, M. H.; Gibson, K. D.; Scheraga, H. A. *J. Biomol. Struct. Dyn.* **1989**, *7*, 421−453.
(42) Schiffer, C. A.; Caldwell, J. W.; Stroud, R. M.; Kollman, P. A. *Protein Sci.* **1992**, *1*, 396−400.
(43) Yamane, T.; Inoue, Y.; Sakurai, M. *Chem. Phys. Lett.* **1998**, *291*, 137−142.
(44) Weiner, S. J.; Singh, U. C.; O'Donnell, T. J.; Kollman, P. A. *J. Am. Chem. Soc.* **1984**, *106*, 6243−6245.
(45) Pettitt, B. M.; Karplus, M. *Chem. Phys. Lett.* **1985**, *121*, 194.
(46) Pettitt, M.; Karplus, M. *J. Phys. Chem.* **1988**, *92*, 3994−3997.
(47) Tobias, D. J.;Brooks, C. L., III. *J. Phys. Chem.* **1992**, *96*, 3864−3870.
(48) Jean-Charles, A.; Nicholls, A.; Sharp, K.; Honig, B.; Tempczyk, A.; Henderson, T. F.; Still, W. C. *J. Am. Chem. Soc.* **1991**, *113*, 1454−1455.
(49) Marrone, T. J.; Gilson, J. A.; MacCammon, J. *J. Phys. Chem.* **1996**, *100*, 1439.
(50) Sharp, K. *J. Comput. Chem.* **1991**, *12*, 454−468.
(51) Farkas, Ö.; Perczel, A.; Marcoccia, J. F.; Hollósi.; Csizmadia, I. G. *J. Mol. Struct. (THEOCHEM)* **1995**, *331*, 27−36.
(52) Perczel, A.; Farkas, Ö.; Csizmadia, I. G. *J. Am. Chem. Soc.* **1996**, *118*, 7809−7817.
(53) Perczel, A.; Farkas, Ö.; Csizmadia, I. G. *J. Comput. Chem.* **1996**, *17*, 821−834.
(54) Frey, R. F.; Coffin, J.; Newton, S. Q.; Ramek, M.; Cheng, V. K. W.; Momany, F. A.; Schäfer, L. *J. Am. Chem. Soc.* **1992**, *114*, 5369−5377.
(55) Case, D. A. In *Conformational Analysis of Medium-Sized Heterocycles*; Glass, R. S., Ed.; VCH Publishers: New York, 1988; pp 1−34.
(56) Head-Gordon, T.; Head-Gordon, M.; Frisch, M. J.; Brooks, C. L., III.; Pople, J. A. *J. Am. Chem. Soc.* **1991**, *113*, 5989−5997.
(57) Bolhuis, P. G.; Dellago, C.; Chandler, D. *Proc. Natl. Acad. Sci. U.S.A.* **2000**, *97*, 5877−5882.
(58) Cornell, W. D.; Cieplak, P.; Bayly, C. I.; Gould, I. R.; Merz, K. M., Jr.; Ferguson, D. M.; Spellmeyer, D. C.; Fox, T.; Caldwell, J. W.; Kollman, P. A. *J. Am. Chem. Soc.* **1995**, *117*, 5179−5197.
(59) Case, D. A.; Pearlman, D. A.; Caldwell, J. W.; Chatham, T. E., III.; Ross. W. S.; Simmerling, C. L.; Darden, T. A.; Merz, K. M.; Stanton, R. V.; Cheng, A. L.; Vincent, J. J.; Crowley, M.; Tsui, V.; Radmer, R. J.; Duan, Y.; Pitera, J.; Massova, I.; Seibel, G. L.; Singh, U. C.; Weiner, P. K.; Kollman, P. A. *AMBER 6*; University of Calformia: San Fransisco, CA, 1999.
(60) Jorgensen, W. L.; Chandrasekhar, J.; Impey, R. W.; Klein, M. L. *J. Chem. Phys.* **1983**, *79*, 926−935.
(61) Berendsen, H. J. C.; Postma, J. P. M.; van Gunsteren, W. F.; DiNola, A.; Haak, J. R. *J. Chem. Phys.* **1984**, *81*, 3684−3690.
(62) Brooks, C. L., III.; Case, D. A. *Chem. Rev.* **1993**, *93*, 2487−2502.
(63) Asakura, T.; Murakami, T. *Macromolecules* **1985**, *18*, 2614−2619.
(64) Asakura, T.; Kahiba, H.; Yoshimizu, H. *Macromolecules* **1988**, *21*, 644−648.
(65) Asakura, T.; Demura, M.; Date, T.; Miyashita, M.; Ogawa, K.; Williamson, M. P. *Biopolymers* **1997**, *41*, 193−203.
(66) Asakura, T.; Iwadate, M.; Demura, M.; Williamson, M. P. *Int. J. Biol. Macromol.* **1991**, *24*, 167−171.
(67) Kataoka, T.; Kobayashi, Y.; Fujiwara, T.; Kyogoku, Y. *Abstract in Symposium of study and utilization of nonmulberry silkworms*; Int. Soc. Nonmulbery Silk., 1981; pp 71−73.
(68) Perczel, A.; Hollosi, M.; Sándor, P.; Fasman, G. D. *Int. J. Peptide Protein Res.* **1993**, *41*, 223−236.
(69) Baker, E. N.; Hubbard, R. E. *Prog. Biophys. Mol. Biol.* **1984**, *44*, 97−179.

MA0209390